# Colored Vertex Models and Interacting Reverse Plane Partitions

Jonah Guse[1], David Jiang[1], and David Keating[1]

[1]Department Of Mathematics, UW Madison, USA

December 21, 2024

**Abstract**

We study the coupling of pairs of reverse plane partitions by assigning a weight to each couple depending on the number of "non-trivial" interactions between the reverse plane partitions. After defining the coupling between pairs of reverse plane partitions we show that they are in bijection with a certain Yang-Baxter integrable colored vertex model. By employing the colored vertex model and Yang-Baxter equation, we are able to compute the generating function for pairs of reverse plane partitions. We also give a bijection between pairs of reverse plane partitions with coupling parameter set to zero and a single reverse plane partition.

# Contents

# 1 Introduction

In this section we give some combinatorial background and define reverse plane partitions. We also introduce the Yang-Baxter integrable five vertex models which we will show are in bijection with the reverse plane partitions. For more background on partitions, plane partitions, and reverse plane partitions, see [8, 2]. The five-vertex models with discuss in this section are closely related to Schur processes [3] and dimer models [4]. For a more general background on vertex models see [6].

## 1.1 Partitions

*Integer partitions* are a very simple and old idea studied in math. In it's essence, it deals with the different ways a number can be split up into different integer parts. For example, 3 can be split up into 3, $2+1$, or $1+1+1$.

**Definition 1.** *An integer partition is a way of writing a positive integer as a sum of other positive integers, where the order of the summands does not matter.*

### 1.1.1 Young Diagram

A *Young diagram* is a pictorial representation of an integer partition. Taking a certain partition $\lambda$, the Young diagram is generated by taking the largest part $\lambda_1$ of $\lambda$ and placing $\lambda_1$ many blocks on the first row, for the second largest part $\lambda_2$ placing $\lambda_2$ many blocks on the second row, and continuing until all parts of the partition have been represented with blocks.

**Example 1.**
*The Young diagrams:*

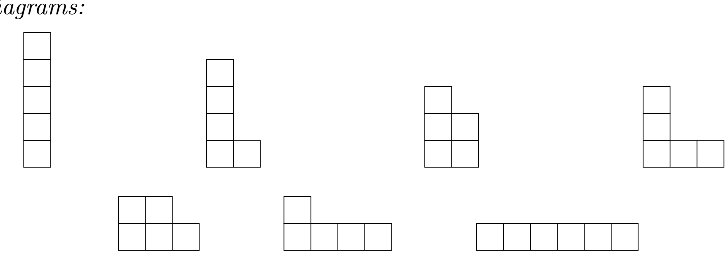

*Correspond with the partitions:*

$5 = 1{+}1{+}1{+}1{+}1$ $\quad$ $5 = 1{+}1{+}1{+}2$ $\quad$ $5 = 1{+}2{+}2$ $\quad$ $5 = 1{+}1{+}3$

$5 = 2+3$ $\quad$ $5 = 1+4$ $\quad$ $5 = 5$

### 1.1.2 Interlacing Partitions

We say that two partitions $\mu$ and $\lambda$ *interlace* if

$$\lambda_1 \geq \mu_1 \geq \lambda_2 \geq \mu_2 \geq \dots$$

and write $\mu \preceq \lambda$. Equivalently, $\mu \preceq \lambda$ if and only if one can get the Young diagram of $\lambda$ from the Young diagram of $\mu$ by adding at most one cell to each column. We say that the two partitions differ by a *horizontal strip*.

**Example 2.** *The partitions* $\mu = (3,2,1,1)$ *and* $\lambda = (4,3,2,1,1)$ *satisfy* $\mu \preceq \lambda$ *since we can get* $\lambda$ *from* $\mu$ *by adding at most one cell to each row. Below we draw the Young diagram of* $\mu$ *in gray* *and the horizontal strip you need to add to get $\lambda$ in white.*

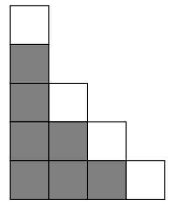

### 1.1.3 Maya Diagram

We can also represent partitions pictorially using diagrams called *Maya diagrams*. To understand Maya diagrams, it is helpful to first represent partitions in *Russian convention*. Russian convention is just a different perspective on Young diagrams, where we rotate the Young diagram 45 degrees to counter-clockwise.

**Example 3.** *We can represent the partition $8 = 4 + 3 + 1$ in the Russian convention as:*

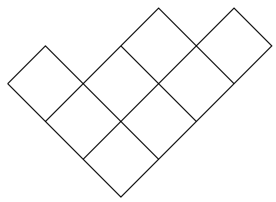

*Notice this is the same as the partition:*

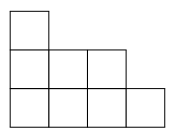

**Definition 2.** Maya diagrams *are a method of representing Young diagrams by a unique string of particles and holes. The way you find the particles and holes is you can imagine you are on the leftmost corner of the Young diagram in Russian convention. You want to following along the top most line. Every time you go diagonally up you add a hole and every time you go diagonally down you add a particle. This sequence of holes and particles is the Maya diagram of the partition.*

**Definition 3.** *There exists a unique point on the Maya diagram where the number of particles to the right of this point is equal to the number of holes to the left of this point. We call this point the* center *of the Maya diagram.*

**Example 4.** *The Maya diagram of the partition $12 = 4 + 3 + 2 + 2 + 1$ is the string of particles and holes underneath the Young diagram below, with the center drawn in red:*

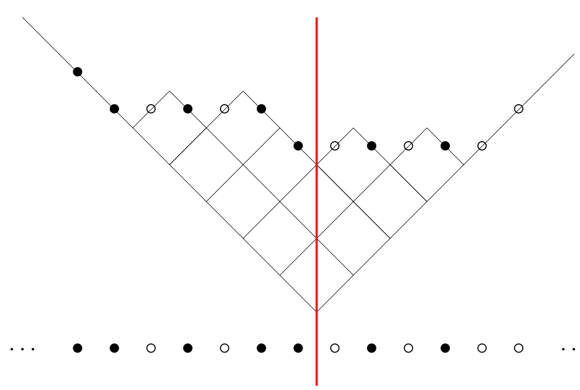

You should define hook-length here.

## 1.2 Plane Partitions

Young diagrams can be thought of as a model for a *one-dimensional partition* because the summands are written in a line: $2 + 2 + 1$. Expanding on this idea, one can define *two-dimension partitions* known as *plane partitions*.

**Definition 4.** *A plane partition of $n$ is a 2-D array of non-negative integers with sum $n$, such that rows are non-increasing from left to right and columns are non-increasing from bottom to top.*

**Example 5.** *These represent some plane partitions of size* 3.

| |
|---|
| 3 |

| |
|---|
| 1 |
| 2 |

| |
|---|
| 1 |
| 1 |
| 1 |

| | |
|---|---|
| 1 | |
| 1 | 1 |

| | | |
|---|---|---|
| 2 | 1 | 1 |

*maybe the last one could be 2,1,1? You don't have an example where the rows aren't constant.*

Plane partitions can be represented in other ways. A natural extension is to represent the plane partition as stacks of cubes corresponding to the numbers written in the arrays. These stacks of cubes can also be thought of as lozenge tilings, where we imagine we are looking at the stacks of cubes from the top right of the Young diagram.

**Example 6.** *Below are the respective lozenge tilings for the plane partitions in Example 5. We color code these lozenge tilings based on the orientation of the lozenges.*

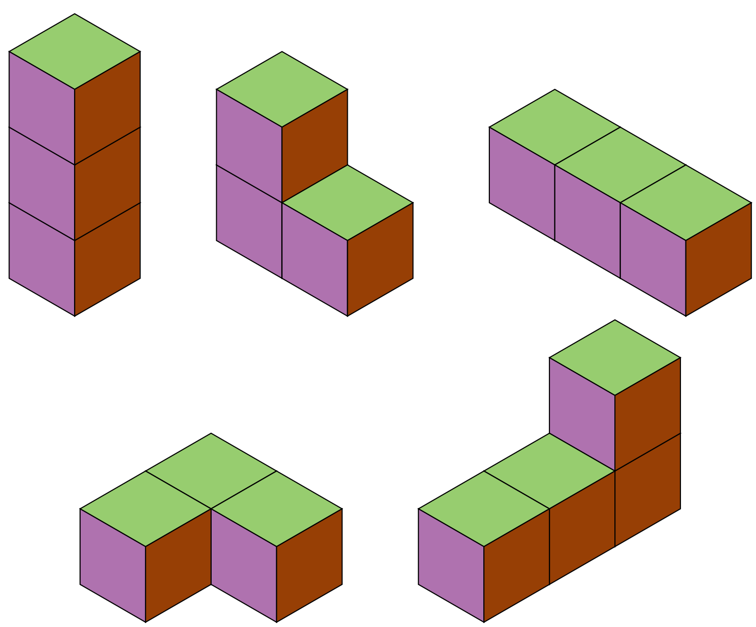

### 1.2.1 Reverse Plane Partitions

**Definition 5.** *Let $\lambda$ be a 1-dimensional partition. A* reverse plane partition *(RPP) of shape $\lambda$ and volume $n$ is an assignment of non-negative integers to the cells in the Young diagram of $\lambda$ such that the integers are non-decreasing from left to right in each row and non-decreasing from bottom to top in each column, and the sum of the integers is $n$.*

**Example 7.** *If $\lambda$ is the partition $9 = 4 + 3 + 2$, then the following is an RPP of shape $\lambda$ and volume* 18*:*

| | | | |
|---|---|---|---|
| 1 | 2 | | |
| 1 | 2 | 4 | |
| 0 | 0 | 3 | 5 |

In particular, there is a nice bijection between RPPs in the shape of a rectangle and PPs, given by rotating the Young diagram by 180 degrees. For example:

| | | | | | | | | |
|---|---|---|---|---|---|---|---|---|
| 3 | 3 | 6 | 6 | $\mapsto$ | 2 | 2 | 0 | 0 |
| 0 | 3 | 3 | 4 | | 4 | 3 | 3 | 0 |
| 0 | 0 | 2 | 2 | | 6 | 6 | 3 | 3 |

Again, we have a bijection between RPPs and lozenge tilings. We can still consider the RPP as stacks of cubes as with plane partitions, but because the inequalities are switched, we must consider lozenge tilings as a view from the bottom left of the Young diagram instead of from the top right, in order to prevent stacks of cubes from obscuring the view of smaller stacks of cubes.

**Example 8.** *The RPP depicted in Example 7 can be represented as the following lozenge tiling:*

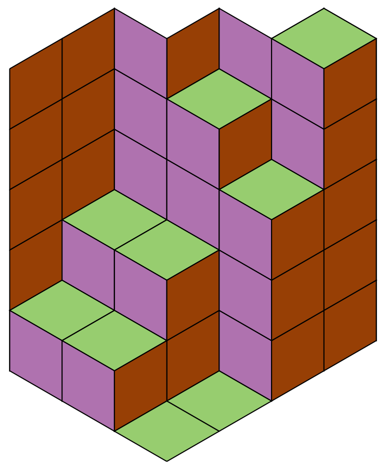

If we fix the shape $\lambda$ the generating function of volume weighted RPP takes a particularly nice form.

**Theorem 1** ([7])**.** *If we fix the shape $\lambda$ of the RPP, then the expression to count the number of possible reverse plane partitions of a given volume can be represented as the generating function*

$$\sum_{\Lambda \in RPP(\lambda)} q^{|\Lambda|} = \prod_{x \in \lambda} \frac{1}{1 - q^{h_\lambda(x)}}$$

*where the product is over all cells of the Young diagram of $\lambda$ and $h_\lambda(x)$ is the hook length of the cell $x$ in $\lambda$.*

## 1.3 Five Vertex Model

Vertex models encompass a large class of models originally arising in statistical physics, but now known to have deep connection to representation theory and, as we shall see, combinatorics. In broad strokes, consider the vertices $(i, j) \in \mathbb{Z}^2$. Suppose we have certain plaquettes we can place over each vertex and that there are restrictions on which plaquettes are allowed at neighboring vertices. Furthermore, we assign weights to the different plaquettes. The type of plaquettes along with the local restrictions and weights define the vertex model.

While the above description is rather vague, it is in part because there are such a wide variety of vertex models that is hard to give a precise definition of what the term means. We would like to stress that the idea that the building blocks of our vertex model only “interact” locally in both the constraints and the weights. For our purposes it will be enough to focus on two types of five-vertex models, where “five” indicates the number of basic plaquettes.

Before we introduce these two types, we will look at how vertex models are generated before we talk about how they are interpreted. Vertex models are created from multiple Maya diagrams where we place the particles and holes onto the coordinate plane at $(i/2, j)$ where $i, j \in \mathbb{Z}$ and they are aligned based on their centers. For the first vertex model, the Maya diagrams are placed in a way in which $\mu \preceq \lambda$ implies that $\lambda$ is on the top and $\mu$ is on bottom. We enforce the constraint that each particle must be connected to the closest particle on top or to the right of itself while the holes will never have a line going through it. For example:

**Example 9.** *Let $\mu = (1,1)$ and $\lambda = (3,1,1)$. Then the row with bottom boundary condition $\mu$ and to boundary condition $\lambda$ (with no paths entering or exiting on the sides) has a unique valid path configuration given by*

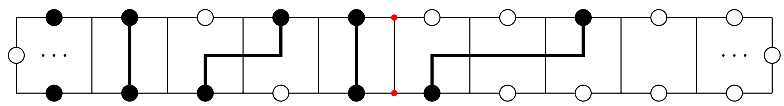

There are only five potential ways for lines to go through a box as depicted in Figure 1. We also assign a weight to each of the five types of vertices, as shown in Figure 1.

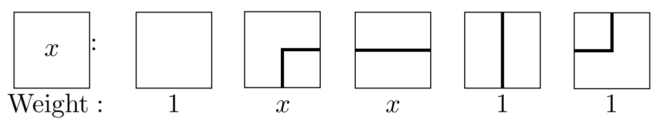


**Figure 1:** White Row Weights

So looking back at our example, this gives us the following weights: $1, x, 1, 1, x, x, 1$, or a total weight of $x^3$.

The other vertex model we have will be shaded gray to denote which one we are looking at. There are slightly different rules for this one. But the weights are essentially the complement of the previous vertex model in which boxes previously having weight 1 are now of weight $x$, and those of weight $x$ are now weight 1. This can be written as follows: $L'_x(\rho) = x\, L_{1/x}(\rho)$ You don't define $L$ anywhere.

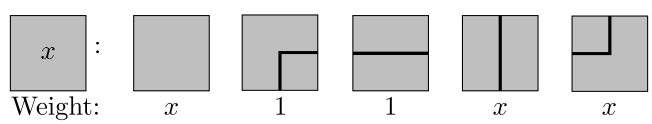


**Figure 2:** Gray Row Weights

**Example 10.** *Let $\mu = (3,1,1)$, $\lambda = (2,1)$, and $k = 4$. Then the row with bottom boundary condition $\mu$ and to boundary condition $\lambda$ has a unique valid path configuration given by*

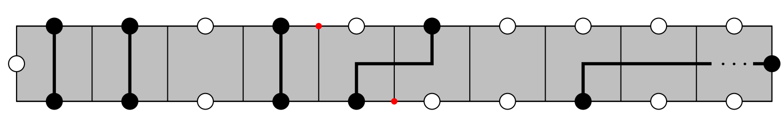

There are four major differences between our gray vertex model and our white vertex model:

- The partition on the bottom boundary is now larger, i.e. $\lambda \preceq \mu$.
- We center the Maya diagram on top one column to the left of the one on the bottom.
- On the right boundary our boundary condition has a path exiting.
- The row is no longer infinite to the left. Do you ever mention how it is not necessary for the white rows to be infinite to the left later?

Somewhere here you should stress that fixing $\lambda$ and $\mu$ the row has a unique path configuration if the partitions interlace correctly and otherwise there is no valid path configuration that satisfies the constraints.

### 1.3.1 Reverse Plane Partition's Vertex Model

By combining several rows of these vertex models, we can create a vertex model representation of the RPP. It will be easiest to see how this is constructed by looking at an example.

**Example 11.** *Consider a RPP of shape $\lambda = (4, 3, 1)$.*

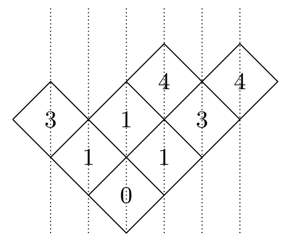


*We can look at the partitions generated by the dotted lines going through the RPP. So in particular we are looking at:*

$$\emptyset \preceq (3) \succeq (1) \preceq (1,0) \preceq (4,1) \succeq (3) \preceq (4) \succeq \emptyset$$

*We can now map this to a path configuration using our vertex model. Whenever we see a $\preceq$ we will have a row of white vertices, while whenever we see a $\succeq$ we put a gray row. The specific partitions tells at what positions the paths cross between the rows. In our example, we have*

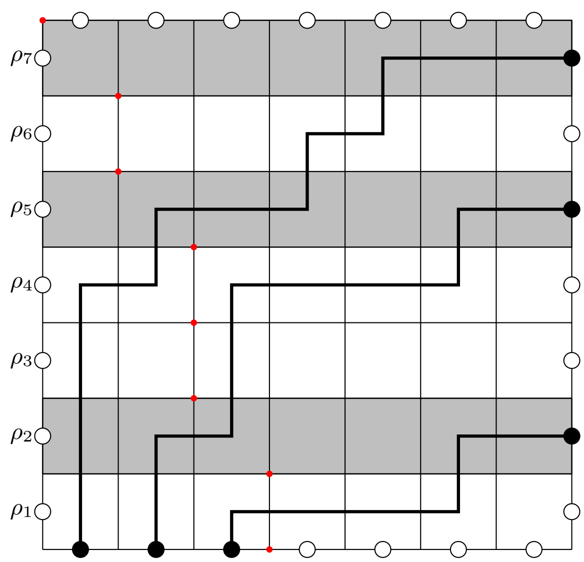


*Note the number of paths is number of non-zero parts of $\lambda$. We could include some number of zero parts in $\lambda$ which would result in extending our domain to the left with columns containing vertical paths. But this is unnecessary.*

*In addition, it is advantageous for us to look at the weights of the diagram which are determined from Figure 1 and 2.*

*By rows, we have that each weight corresponds to: Should have $L'$s? Also you haven't defined* *the Ls. Is $L(\rho)$ the weight of a row or a vertex?*

$$L(\rho_1) : 1 \cdot 1 \cdot x \cdot x \cdot x \cdot 1 \cdot 1 = x^3$$
$$L(\rho_2) : x \cdot 1 \cdot x \cdot x \cdot x \cdot 1 \cdot 1 = x^4$$
$$L(\rho_3) : 1 \cdot 1 \cdot 1 \cdot 1 \cdot 1 \cdot 1 \cdot 1 = 1$$
$$L(\rho_4) : x \cdot 1 \cdot x \cdot x \cdot x \cdot 1 \cdot 1 = x^3$$
$$L(\rho_5) : x \cdot 1 \cdot 1 \cdot x \cdot x \cdot 1 \cdot 1 = x^3$$
$$L(\rho_6) : 1 \cdot 1 \cdot 1 \cdot x \cdot 1 \cdot 1 \cdot 1 = x$$
$$L(\rho_7) : x \cdot x \cdot x \cdot x \cdot 1 \cdot 1 \cdot 1 = x^3$$
$$L(\rho) = x^3 \cdot x^4 \cdot 1 \cdot x^3 \cdot x^3 \cdot x \cdot x^3 = x^{17}$$

One can check that the above gives a bijection between reverse plane partitions of shape $\lambda$ and path configuration of a vertex model in which the number and type of rows is determined by $\lambda$. It might be nice to say exactly how the partition determines the rows. You should define the weight of a configuration $w(\mathcal{C})$ here maybe. (ie its the product of the weight of each vertex in the configuration)

Recall that the vertex models comes with weights, in which we have a choice of parameter for each row. We would like to choose these parameters so that the total weight of the path configuration is equal to q to the volume of the reverse plane partition

**Theorem 2.** *Let $\Lambda$ be a reverse plane partition and $\ell(\lambda)$ be the number of non-zero parts of $\lambda$. Let $\mathcal{C}$ be the corresponding path configuration under the bijection described above. Then if one chooses the weights parameters of the vertex model to be $x_i = q^{\pm i}$ where we take $+$ for a gray row and $-$ for a white row, we have*

$$q^{vol(\Lambda)} = w(\mathcal{C}) \cdot A_\lambda(q)$$

*where $A_\lambda(q) = q^{\sum_{i=1}^{\ell(\lambda)}(\lambda_i - i + \ell(\lambda))(i-1)}$ is completely determined by the shape $\lambda$ and is independent of the specific configuration.*

## 1.4 Vertex Model and Lozenge Tilings Bijection

This subsection should go at the end of Section 1. Then Section 2 can be all about introducing the multicolored model.

We can go back and forth between reverse plane partitions and lozenge tilings by considering both as stacks of cubes.

Because we can also go back and forth between reverse plane partitions and vertex diagrams, we might expect that we can find a nice bijection between vertex diagrams and lozenge tilings.

**Example 12.** *We will continue Example 11 and use this running example while explaining this bijection between vertex diagrams and lozenge tilings. Here have the RPP of shape $\lambda = (4, 3, 1)$*

*given in Example 11, shown as both a vertex model and a lozenge tiling.*

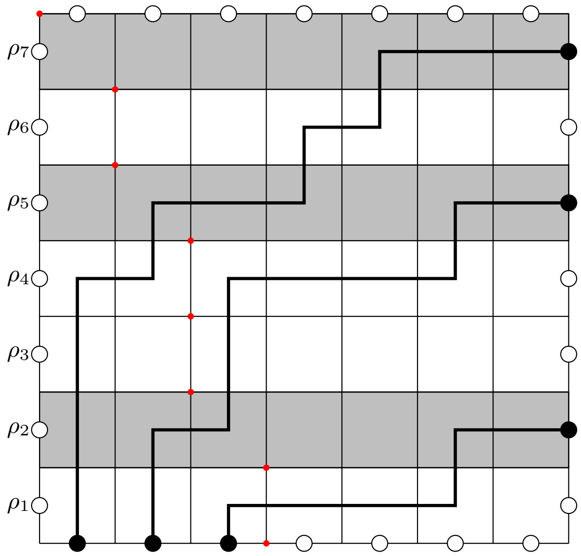


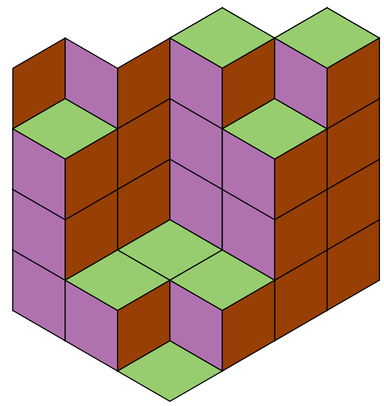

We can split a lozenge tiling up into columns, each the same width as a orchid what? lozenge. Considering the lozenge tiling as stacks of cubes ~~and looking at the top view of these stacks~~, each column corresponds to exactly one particle or hole in the Maya diagram for the shape of this reverse plane partition this senttence is confusing, do you mean the back wall of the stack of cube?. Then we can assign each column of the lozenge tiling a color, gray or white, based on whether the column corresponds to a particle or hole, respectively, in the Maya diagram.

This suggests that each column (left to right) of the lozenge tiling corresponds to a row (bottom to top, respectively) of the vertex diagram, where the gray/white columns in the lozenge tiling correspond to gray/white rows in the vertex diagram.

It is helpful to distinguish between the different orientations and positions of lozenges. For this purpose, we will call the "left-leaning" lozenge (pictured in orchid) "lozenge $a$", the "right-leaning" lozenge (pictured in raw sienna) "lozenge $b$", and the "horizontal" lozenge (pictured in yellow green) "lozenge $c$". Because $c$ lozenges lie in multiple columns we will further distinguish between two types of $c$ lozenges when we are working in a particular column. If the lozenge is partially in this column and partially to the right of the column, we will call it $c_r$. If the lozenge is partially to the left of the column, we will call it $c_l$.

**Definition 6.**

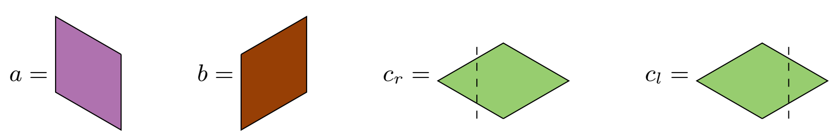


We can now look at the right boundary of the first (leftmost) column in a lozenge tiling. The first column will consist of 0 or more instances of lozenge $a$, then exactly 1 lozenge $c_r$, then arbitrarily many instances of lozenge $b$ representing the back wall. We can place a hole on the right boundary of this column on the right side of any $a$ or $b$ lozenge, and a particle on this boundary at the center of the $c_r$ lozenge. We continue to do this for each column and draw all the holes and particles corresponding to the lozenges.

**Example 13.** *We will look at every column and subsequently fill in the corresponding holes and particles based on the way we described it.*

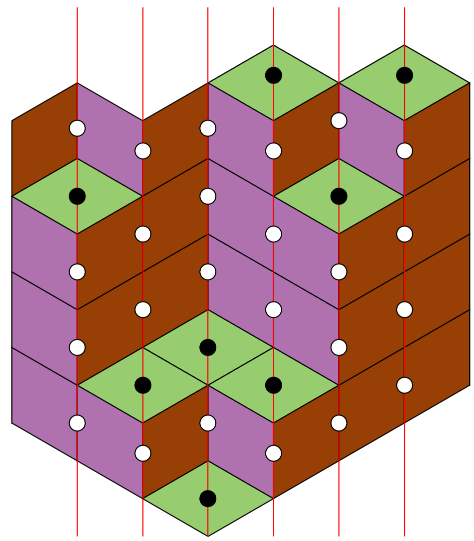

Reword this paragraph

If we rotate these holes and particle clockwise a quarter turn so that bottom-to-top becomes left-to-right, we have a Maya diagram. Because this column boundary bisects the $c_r$ lozenge and considering the top view of the corresponding cube stacks, we can tell that this Maya diagram corresponds to the partition comprising the first column of the RPP in the Russian convention. In the same way, Maya diagrams built along other column boundaries correspond to Maya diagrams of each column of the RPP in the Russian convention.

**Example 14.** *After rotating the previous example in the way that we have described, we get the vertex model that we depicted earlier*

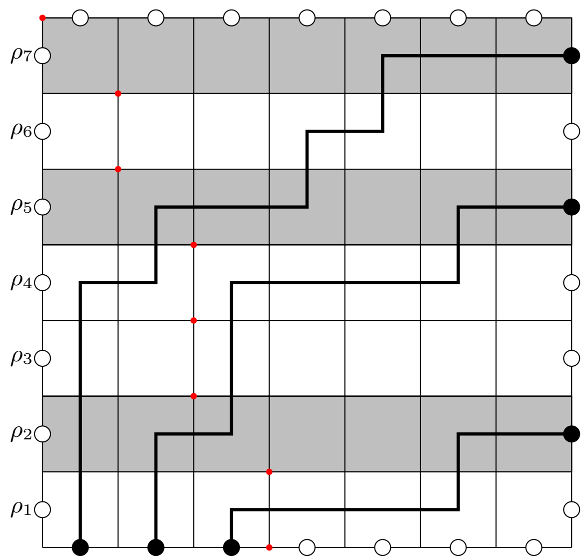


But it is exactly these Maya diagrams which define the boundary conditions between rows in the vertex diagram. Therefore, the relative locations of $a$, $b$, and $c$ tiles in the lozenge tiling almost directly translate into the boundary conditions for the vertex diagram.

In fact, we can connect lozenge tilings to vertex diagrams even more closely. Consider any column in a lozenge tiling. Any instances of lozenge $a$ can be grouped into disjoint "runs" of consecutive $a$ lozenges. These runs must occur at the beginning (bottom) of the sequence or immediately after a $c_l$ lozenge, and be immediately followed by a $c_r$ lozenge.

In either case, we can look on the left boundary of this column, where the $c_l$ (possibly from the floor) creates a particle and the left edge of each $a$ must be a hole (since a $c$ lozenge would not fit there). Then on the right boundary, the right edge of each $a$ must be a hole and the $c_r$ creates a particle. We then see that the number of $a$ lozenges in a run corresponds to the distance we slide a particle to the right in one row of the vertex diagram. In a white column, this means each $a$ tile contributes a factor of $x$.

Similarly, any run of $b$ lozenges must be preceded by a $c_r$, representing a particle at the top of a row in a vertex diagram, and followed by a $c_l$, representing a particle at the bottom of a row in a vertex diagram. Then each $b$ corresponds to a hole at the top and bottom of a row in the vertex diagram between a path leaving the row and a new path entering, i.e. an empty box in the vertex diagram. In a gray row, this means each $b$ tile contributes a factor of $x$.

Similarly, any $c_r$ tile in a gray column corresponds to a particle at the top of a row in the vertex diagram, so it contributes a factor of $x$. However, since all RPPs of the same shape have the same top view and thus equal numbers of $c_r$ tiles in any given column. In other words, the factors of $x$ contributed from the $c_r$ tiles can be considered trivial and we can focus on the weights from the other tiles.
Add diagram detailing the previous 3 paragraphs

### 1.4.1 Yang Baxter Equation

The advantage of using the vertex model framework is that our vertex models are Yang-Baxter integrable, that is, the satisfy the Yang-Baxter equation (YBE). To describe the (YBE) we will also need cross vertices, with weights defined as shown here:

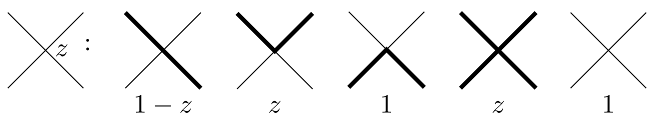


**Figure 3:** Cross Weights

We can attach these crosses to two white vertices and we have the following equality of partition functions

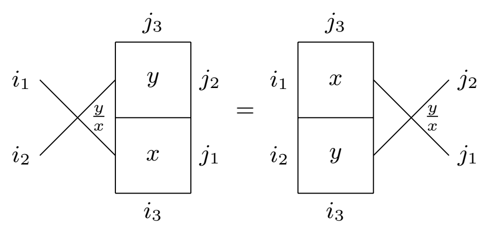


where $i_1, i_2, i_3, j_1, j_2, j_3 \in \{0, 1\}$ with 1 indicated a path present at that boundary and 0 indicating no path. In other words, for any given boundary conditions $i_1, i_2, i_3, j_1, j_2, j_3$, the sum of the weights of all path configurations satisfying the boundary conditions on the LHS above is equal to the sum of weights of all path configurations satisfying the same boundary conditions on the RHS. This can be checked by exhaustively checking each case.

**Example 15.** *Suppose we set $i_1 = j_2 = 1$ and the rest to zero. Then the YBE says we have the* *following equality of partition functions:*

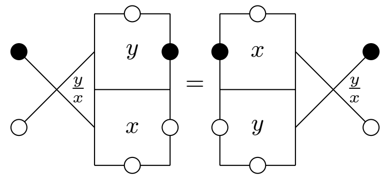


*Explicitly writing the sum over path configurations, this becomes*

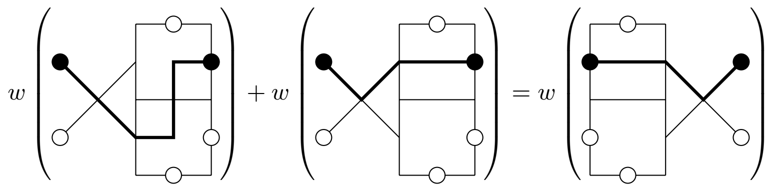


*where we see there are two ways to fill in the paths on the left but only one on the right. Computing the weights we have*

$$\textit{LHS:} \qquad \left(1 - \frac{y}{x}\right) \cdot y + \frac{y}{x} \cdot y = y$$

$$\textit{RHS:} \qquad x \cdot \frac{y}{x} = y$$

*which are in fact equal.*

This result is very useful because we can attach an empty cross with weight 1 to the left end of two long rows of white vertices, then apply YBE repeatedly to swap the vertices in these rows one by one until they are all swapped, and we can sometimes control the total weight of the cross at the right end of this row, so we may be able to remove it with a predictable cost. It would be really helpful if there was an example of the row swapping.

The "trivial" factors of $x$ described in the previous section are extremely useful. This makes the weight of a gray vertex with parameter $x$ equal to $x$ times the weight of a white vertex with parameter $1/x$, regardless of the shape of the path in this vertex. I don't know what the previous sentence is trying to say. Then YBE still holds if we replace one or both of the white vertices with gray vertices and correct weight parameters accordingly (i.e. we replace a white vertex having parameter $x$ by a gray vertex having parameter $1/x$).

I think without a proof of Theorem 1 its hard to understand the point of this section.

Using Theorem 2 and the YBE we can give a quick proof of Theorem 1.

*Proof.* do a bunch of row swaps. keep track of the weights. □

# 2 Multicolored vertex models and overlapping RPP

We have shown that reverse plane partitions can be represented both by a vertex model and a lozenge diagram. We now generalize the vertex models of the previous section by introducing the multicolored vertex model first introduced in [5, 1]. This model allows us to create a bijection from a 2-colored vertex model to a coupling of 2 overlapping RPPs.

## 2.1 Colored Vertex Model

Here we introduce the two-color vertex models we will consider.

### 2.1.1 White Rows

We will first look at the corresponding white rows that we also had for the one color case.
Note the weights we have assigned to these vertices. The obvious choice is to say that the weight of each vertex is the product of the weight of each color from Figure 1. However, we would like to add an interaction between the colors. In order to do this, it is convenient to give an ordering to

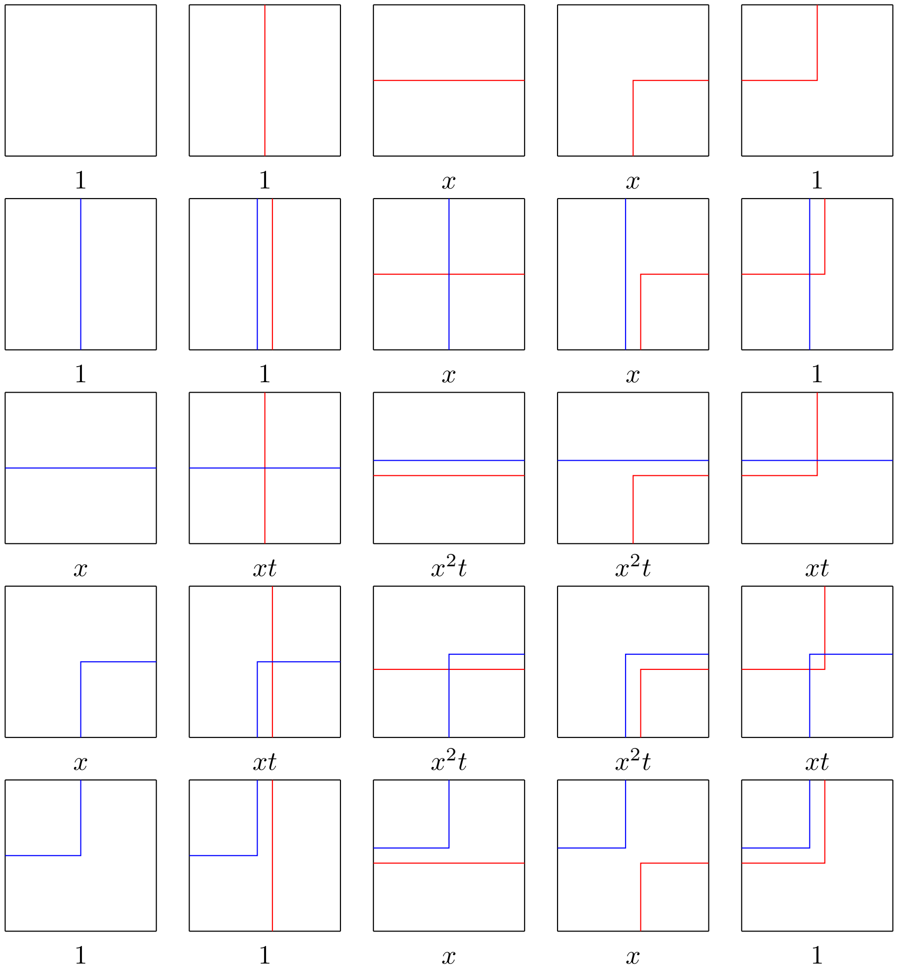


**Figure 4:** White Row Colored Weights

the colors: in the two-color case we can just choose blue to be smaller than red. Then the weights we have above can be written as:

$$L^{(2)}_{x;t}((v_b, v_r)) = L_{xt^{\delta_1}}(v_b)L_x(v_r), \qquad \delta_1 = \mathbf{1}(\text{red is present})$$

Note when $t = 1$ this reduces to the product of the weights.

**Remark 1.** *It's reasonable to ask why we make this choice of coupling. As we will see in a moment, these weights still satisfy a Yang-Baxter equation which, as we've seen, gives us a powerful tool for studying the model.*

**Example 16.** *We will consider rows of vertices just as before. Now our boundary conditions for the rows will be indexed by a pair of partitions: one for blue and one for red. As an example consider the row*

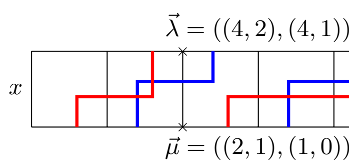


*It has weight $x^7t^3$.*

### 2.1.2 YBE for Colored Vertex Model

This vertex model still solves a version of the Yang-Baxter equation. In the one-color case, the cross weights were given by

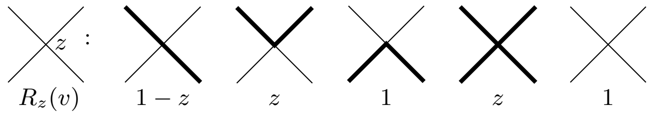


Since we've changed the vertex weights we must change the cross weights as well. The new weights are given by

$$R^{(2)}_{z;t}((v_b, v_r)) = R_{z/t^{r_1}}(v_b) R_z(v_r)$$

where $r_1 = \mathbf{1}$ (red path looks like 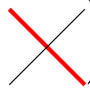).

For example, we have

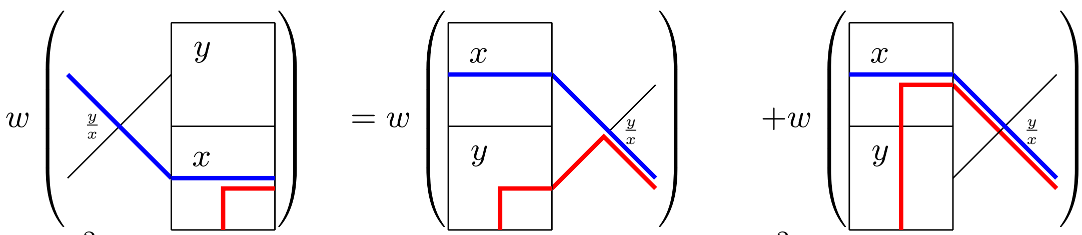


$$x^2 t(1 - y/x) \qquad = xy(1 - y/x) \qquad + x^2 t(1 - y/x)(1 - y/(xt))$$

Should I mention the YBE that Keating mentioned in his notes on colored vertex models? Otherwise the remark is useless, and I think it is slightly confusing why we add a parameter of t

### 2.1.3 Gray Rows

Similarly, these would be the vertex interactions for the gray rows: Remember previously for the one-color case we had the relation between the weights for white rows vs gray rows was given as:

$$L'_x(\rho) = x\, L_{1/x}(\rho)$$

In the 2-color case this becomes

$$(L')^{(2)}_{x;t}(\vec{v}) = x^2 t\, L^{(2)}_{\bar{x};t}(\vec{v}), \qquad \bar{x} = \frac{1}{xt}$$

One can show that the contribution of color $i$ (1=blue, 2=red) can be written as

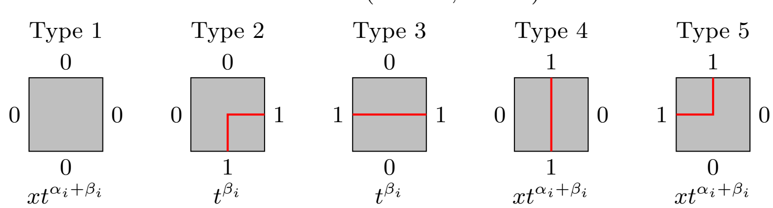


where

$$\alpha_i = \#\text{ colors greater than } i \text{ of Type 1},$$
$$\beta_i = \#\text{ colors greater than } i \text{ of Type 4 or 5}.$$

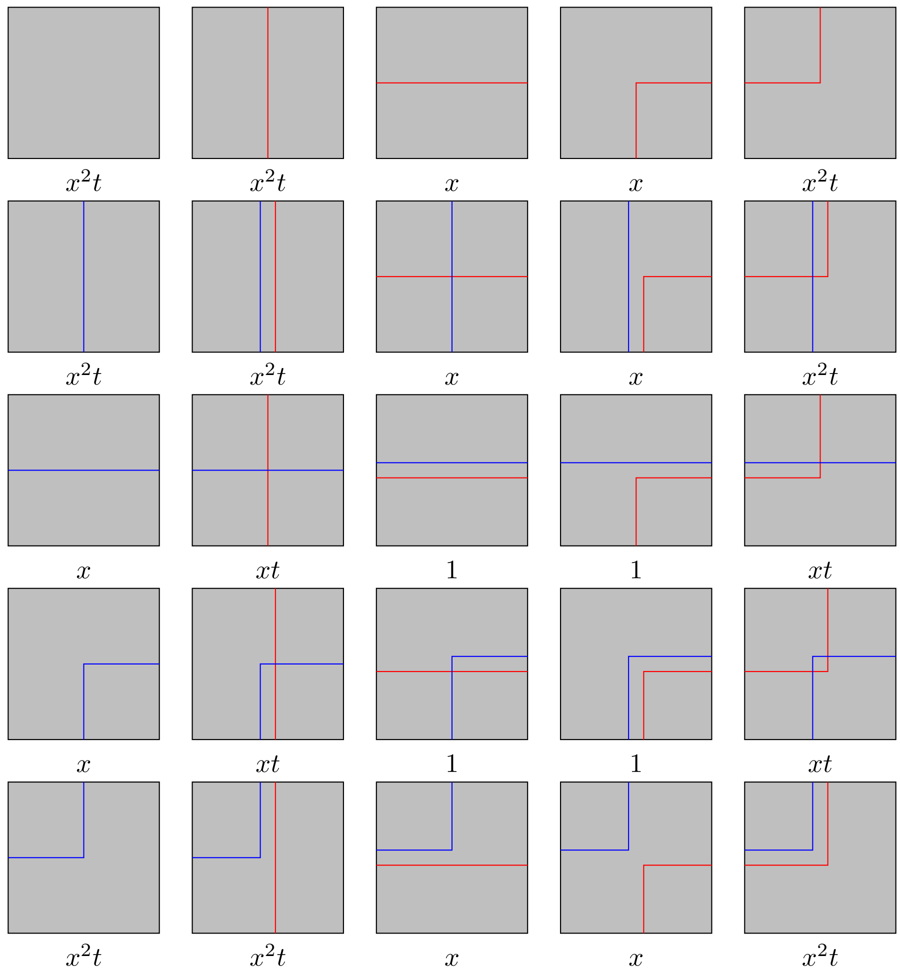


**Figure 5:** Gray Row Colored Weights

**Example 17.** *We can consider a row of this vertex model with boundary conditions on the top and bottom indexed by pairs of partitions. Consider*

$$\vec{\lambda} = ((1, 1), (1, 1))$$

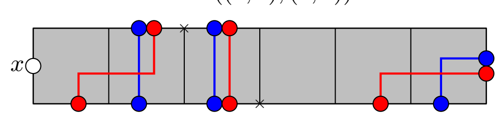


$$\vec{\mu} = ((3, 1, 1), (2, 1, 0))$$

*which has weight* $x^8t^3$*.*

We can now put together our white rows and gray rows in a similar fashion as we did for the one color case. The overlapping is simply just overlaying the one color vertex diagrams for two different RPPs on top of each other. The colors are assigned to each RPP based on your own decision, and the weights are calculated by looking at the weight of each separate box. A good example is shown in **??**. This paragraph is confusing and maybe unecessary. Or could be moved to be the intro paragraph to the next subsection.

## 2.2 Overlapping RPPs

~~We know how this newly defined vertex model works for reverse plane partitions. As alluded to, this is to allow for us to overlap pairs of RPPs.~~ Put a better version of the last paragraph of the previous section here. It makes most sense to explain it via an example:

**Example 18.** *We will use the following RPPs with their corresponding lozenge tilings:*

| | | |
|---|---|---|
| 2 | | |
| 1 | 3 | |
| 0 | 1 | 1 |

| | | |
|---|---|---|
| 2 | | |
| 1 | 2 | |
| 1 | 2 | 3 |

**Figure 6:** Example RPPs

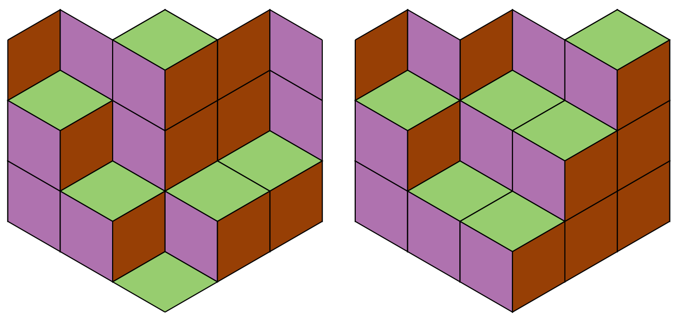

**Figure 7:** Example Lozenge Tiling

*This will be the example of the pair of RPP that we will use. We must define some sort of ordering between the RPPs. This is not defined based on the RPPs themselves, but rather just what we define. Canonically we had defined that the red lines in our vertex model is our "larger" RPP. In this case, we will additionally canonically represent the right lozenge tiling as the red lines.*

*Since the centers of the vertex models are defined based on the 2D shape of the RPP, it is guaranteed that the two RPPs can be overlaid onto the same vertex model with correct dimensions. We can then cross reference with Figures 2 and 1 to get the total weight of the overlap between two RPPs. The weight and the vertex model are shown in Figure 8.*

You could stress here that this gives a combinatorial bijection between the 2-colored vertex model and overlapping RPPs, but we still need to work out how the vertex model weights map to RPP weights.

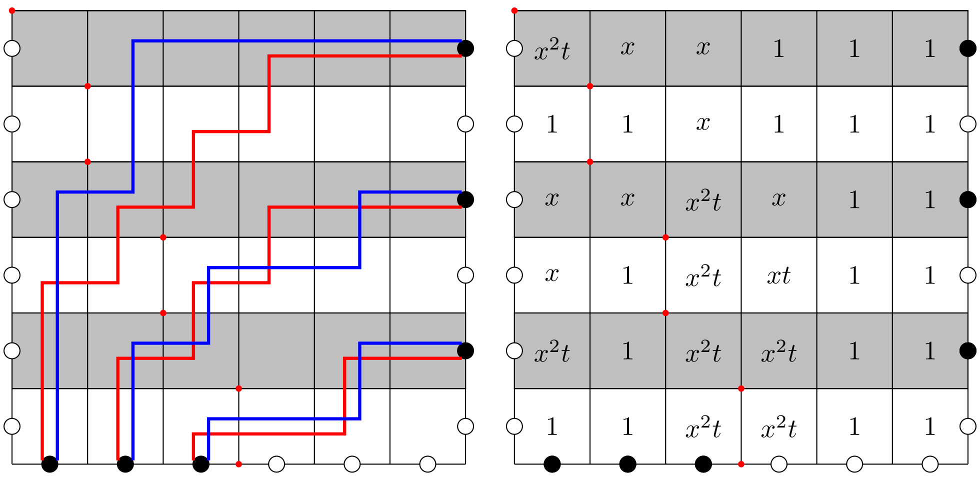


**Figure 8:** Example Vertex Model and Corresponding Weights

# 3 Understanding Weights

This all could be part of Section 2.

We have now represented the main model that we are looking at, the paired RPP. We will first understand combinatorially what our model depicts. What we will first do for this is to explain what exactly the weight represents, since we will be heavily using the combinatorial aspects of the weights when proving the generating function.

## 3.1 Trivial Weights

The weight that we compute for the overlapped RPPs will result in something we call "trivial" weights. They are considered trivial because they are forced in every such RPP with that certain shape, so they don't necessarily give us any information about the RPPs and must just be there regardless. Trivial $t$'s are a bit more interesting because they are not present in the one-color vertex diagrams, while the $x$'s are essentially an extension of the one-color case.

### 3.1.1 $t$'s

The first thing that should be discussed before we look at the lozenge tilings are when we are forced to have a factor of $t$ in our weights. We will denote these as trivial $t$'s, and they are determined just by the number of gray rows that we have. But the number of gray rows is equivalent to the number of paths that we are, which corresponds to the number of non-zero parts of our RPP.

**Lemma 3.** *The contribution of trivial $t$'s given $\ell$ many paths in the vertex diagram is equivalent to $t^{\frac{\ell(\ell-1)}{2}}$.*

*Proof.* At the start of our vertex diagram we will have $n$ many "paths". At each gray row, one path will be retired. This means that we will have $\ell - 1$ many gray rows exit through the top. Since by the way the weights are defined in Figure 5, anytime a red path exits through the top we will get a contribution of a $t$. Since each time we are going to decrement by 1 path, we notice that these are the triangular numbers, so the amount of trivial $t$'s is equivalent to $\frac{\ell(\ell-1)}{2}$. □

### 3.1.2 $x$'s

We can do something similar to what we did for the $t$'s to determine what the exponent of our trivial factors of $x$ should be. Similarly, all of our trivial cases come from the gray row and they come from the same vertex boxes that contribute trivial $t$'s. However, it isn't as simple as computing the triangular number this time as the exponent of the trivial vertex boxes can be 1 or 2.

## 3.2 Non-Trivial Weights

Now that we've cleared up the forced weights or trivial weights, we will now discuss the actual factors that we care about. To do so, it will be more insightful to actually look at the lozenge tilings/cube stacks as they give us a more tangible idea with what we are working with.

### 3.2.1 $t$'s

Now that we have dealt with our trivial $t$'s, we will look at the actually important $t$'s.

Recall our notation of orchid lozenges being denoted $a$, raw sienna lozenges $b$, and yellow green lozenges being either $c_r$ or $c_l$, where $c_r$ is when the yellow green lozenge protrudes to the right, and $c_l$ protrudes to the left. Additionally, we will define the notation of a lozenge being "on top" as being the red line and blue as being the lozenge being on the bottom.

The way we will think about these interactions is by laying the lozenge tilings on top of each like what we did for the colored vertex diagrams. Then we look at how the various lozenge's interact with each other.

**Definition 7.** *The following interactions results in the contribution of a $t$ when looking at their lozenge tilings overlapped.*

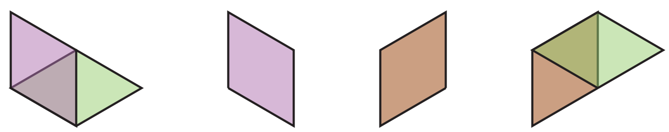

**Figure 9:** $t$ Contributing Interactions

### 3.2.2 $x$'s

The non-trivial $x$'s are just equivalent to the total volume of both of the partitions $\Lambda$ and $\Lambda'$. This notion of volume is just how many cubes are stacked in their corresponding cube diagram. The non-trivial $x$'s are considerably simpler to understand than the $t$'s. This makes sense given that the $t$'s were introduced in order to explain the interaction between $\Lambda$ and $\Lambda'$ while the $x$ corresponds directly with what we were given in the one-color vertex model, so we shouldn't expect there to be anything special when overlaying the RPPs.

**Example 19.** *The weights make a lot more sense when looking at the actual cube stacks. It might help to look at this example to understand exactly what we are talking about.*

*We will use the example depicted in Section 2.2 to exemplify the previously defined ideas of weights in coupled RPPs.*

*Summing up the weights in Figure 8 we get that we have 9 total $t$'s. Recall that since we have 3 gray rows, this means that we will have 3 $t$'s which are trivial. Which means that we should expect* 6 *$t$'s that are contributed from the interactions defined in the previous section.*

*Looking at the first column of 7 we notice that we have the interaction of two $a$ lozenges which is one of the interactions detailed in figure 9. This interaction is highlighted by a red circle inside the* *lozenge:*

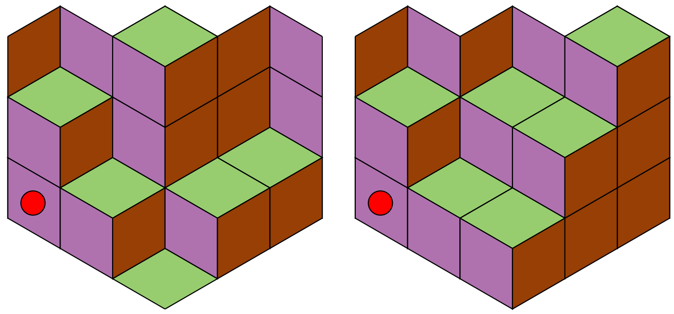

*These lozenges contribute* $2$ *factors of* $t$ *into our weight, meaning we now have* $4$ *more to find. This corresponds to the first row of our vertex diagram, which had a contribution of* $2$ $t$*'s to our total weight. This makes sense since we shouldn't have a trivial factor since we are not in a gray row.*

*We will now look at the next column, looking for the interactions described, we notice that we only get one interaction of* $b$ *on* $b$ *(red circles) and none of* $b$ *on top of* $c_r$*.*

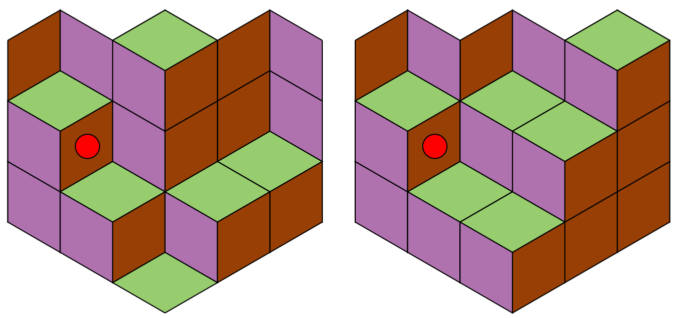

*We can now continuously apply the rules that we have previously defined with the other columns and find the total contributions of non-trival* $t$*'s to our weight.*

*So at the end we are left with* $6$ *interactions that all contribute a factor of* $t$ *to our weight. Which corresponds to our weight when we disregard the trivial factors. So this is a good demonstration as to where the* $t$*'s come from.*

*We've already demonstrated that calculating the number of* $x$*'s is not difficult for the lozenge tilings. Looking at the lozenge tilings:*

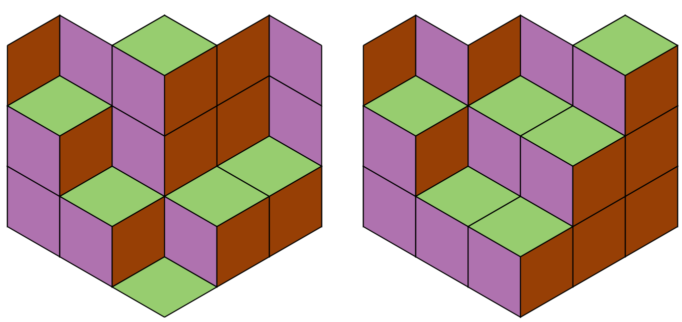

*We notice that we have a total volume of* $19$*. Given that the total contribution of* $x$ *is* $x^{24}$*, that means that we get our expected* $5$ *trivial factors of* $x$ *from the gray rows.*

*I think the previous section is suppose to have a bijection between pairs of RPPs and two-colored 5V models. This should be given as a proposition/theorem with a proof (or at least a sketch).*

# 4 Pairs of Reverse Plane Partitions and Vertex Models

## 4.1 Generating Function for Pairs of Reverse Plane Partitions

Our goal in this section is to prove the following theorem:

**Theorem 4.** *Given two RPPs $\Lambda, \Lambda'$, define $g(\Lambda, \Lambda')$ to be the number of overlaps of the types described in Figure 9 when we overlay the lozenge tiling of $\Lambda$ over the lozenge tiling of $\Lambda'$. Then for any fixed $\lambda$:*

$$\sum_{\Lambda, \Lambda' \in RPP(\lambda)} x^{vol(\Lambda)+vol(\Lambda')} t^{g(\Lambda,\Lambda')} = \prod_{s \in \lambda} \frac{1}{(1 - x^{h_\lambda(s)})(1 - x^{h_\lambda(s)} t)}$$

*Proof.* Because the weight of a pair of paths in a gray box with parameter $x$ is equal to $(x^2 t)$ times the weight of the same paths in a white box with parameter $1/(xt)$, and because the YBE holds for white boxes, we obtain the YBE for a white box on top of a grey box as shown below:

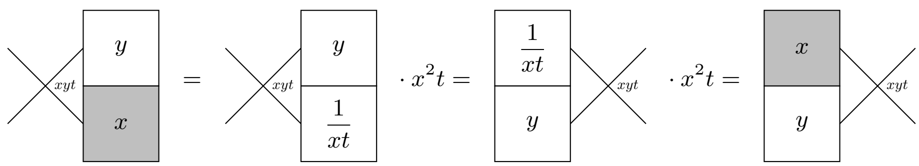


Given some partition shape $\lambda$, the weight of every pair of reverse plane partitions of shape $\lambda$ contains the trivial factor:

$$A_\lambda(x, t) = x^{2 \sum_{i=1}^{\ell(\lambda)} (\lambda_i - i + \ell(\lambda))(i-1)} t^{\frac{\ell(\lambda)(\ell(\lambda)-1)}{2}}$$

where $\ell(\lambda)$ denotes the number of parts in the partition $\lambda$, i.e. the number of rows in the Young diagram of $\lambda$, and $\lambda_i$ denotes the value of the $i$th part of $\lambda$, i.e. the length of the $i$th row from the bottom in the Young diagram of $\lambda$. Then we want to describe the generating function for pairs of plane partitions, which can be written as

$$z_\lambda(x, t) = A_\lambda(x, t) \sum_{\Lambda, \Lambda' \in RPP(\lambda)} x^{vol(\Lambda)+vol(\Lambda')} t^{g(\Lambda,\Lambda')}$$

But by the bijection given in the previous section, $z_\lambda(x, t)$ will also be the sum of the weights of all possible pairs of paths in the two-color five-vertex model with boundary conditions determined by $\lambda$, where the parameters of a vertex in the $i$th row from the bottom are $(x^{-i}, t)$ if the row is white and $(x^i, t)$ if the row is gray.

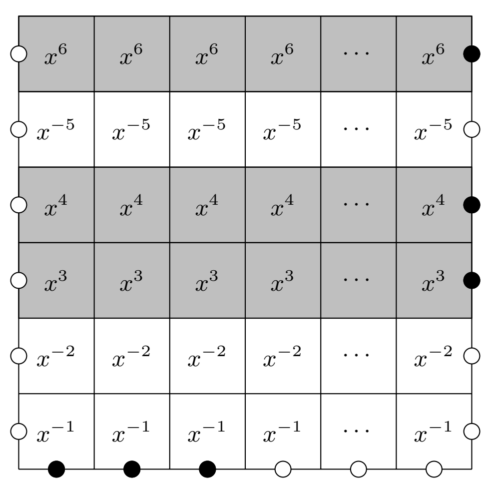


Then we want to determine the sum of the weights of all possible pairs of paths in this two-color vertex model. We can start with all of the gray rows on the bottom and all of the white rows on the top, so that there is only one possible configuration of paths, and we can calculate its weight to be $A_\lambda(x,t)$.

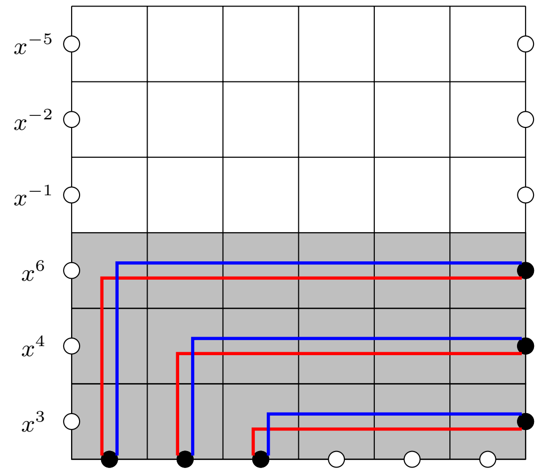


Then we can add a weightless cross with parameter $x^{h_\lambda(s)}t$ to the left edge of our grid, where $h_\lambda(s)$ is the hook length of a square $s \in \lambda$, determined by the grey row and the white row we are switching I don't think it is obvious at all that the hook length comes in to play here.. Then we use YBE to slide this cross across, swapping the grey and white row as we go while not varying the sum of the weights of all possible paths in the grid. You didn't describe any of this in the one-color case. Add diagram and example to explain, and then reword this paragraph to not be about the one-color case

Then when the cross is at the right end of the row, we cannot remove it for free because it is no longer weightless. There are four possible path configurations for this cross, but three of them require the grid to have a weight which converges to 0 for $|x| < 1$. The only configuration which can contribute a nonzero weight is the one where both colors have a downward diagonal path in the cross. Then the weight of the cross is $(1 - \frac{x^{h_\lambda(s)}t}{t})(1 - x^{h_\lambda(s)}t)$, so in order to remove this cross, we must multiply by this weight. Continue previous example here for the picture

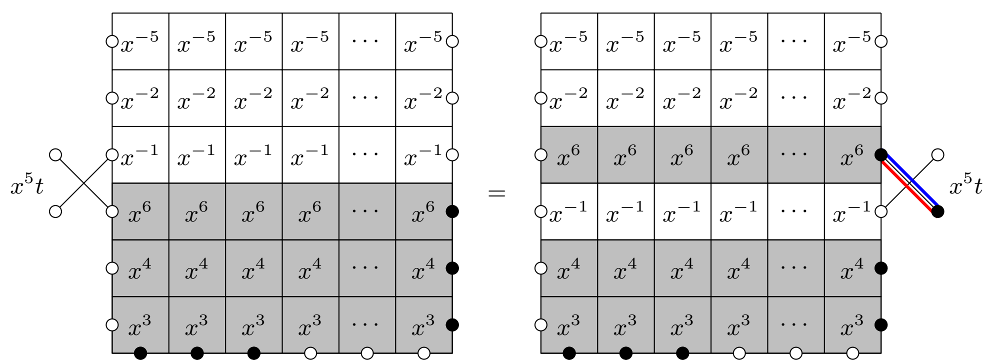

=
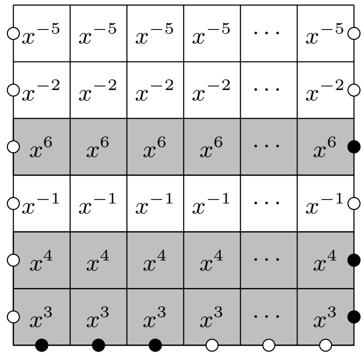

$\cdot(1-x^5)(1-x^5t)$

Repeating this process until the right edge boundary condition matches the Maya diagram of $\lambda$, we get that

$$z_\lambda(x,t)\prod_{s\in\lambda}(1-x^{h_\lambda(s)})(1-x^{h_\lambda(s)}t) = A_\lambda(x,t)$$

But then dividing on both sides gives us a new expression for $z_\lambda(x,t)$:

$$z_\lambda(x,t) = A_\lambda(x,t)\prod_{s\in\lambda}\frac{1}{(1-x^{h_\lambda(s)})(1-x^{h_\lambda(s)}t)}$$

Setting this equal to our other expression for $z_\lambda(x,t)$ and dividing by $A_\lambda(x,t)$ gives us:

$$\sum_{\Lambda,\Lambda'\in RPP(\lambda)} x^{vol(\Lambda)+vol(\Lambda')}t^{g(\Lambda,\Lambda')} = \prod_{s\in\lambda}\frac{1}{(1-x^{h_\lambda(s)})(1-x^{h_\lambda(s)}t)}$$

□

## 4.2 Take $t \to 0$

We can now more easily prove the following theorem.

**Theorem 5.** *The number of pairs of reverse plane partitions of the same shape $\Lambda, \Lambda' \in RPP(\lambda)$ satisfying $g(\Lambda,\Lambda') = 0$ (i.e. the number of $t$-overlaps is 0) and having total volume $n$ is equal to the number of reverse plane partitions of shape $\lambda$ and total volume $n$, for any integer $n \geq 0$.*

*Proof.* We start with the result from Theorem 4:

$$\sum_{\Lambda,\Lambda'\in RPP(\lambda)} x^{vol(\Lambda)+vol(\Lambda')}t^{g(\Lambda,\Lambda')} = \prod_{s\in\lambda}\frac{1}{(1-x^{h_\lambda(s)})(1-x^{h_\lambda(s)}t)}$$

Now we take the limit as $t$ approaches 0 on both sides. On the LHS, all terms containing a positive power of $t$ vanish. On the RHS, the second factor in the denominator approaches 1. Thus, we obtain:

$$\sum_{\Lambda,\Lambda'\in RPP(\lambda),g(\Lambda,\Lambda')=0} x^{vol(\Lambda)+vol(\Lambda')} = \prod_{s\in\lambda}\frac{1}{1-x^{h_\lambda(s)}}$$

The LHS is now the generating function for pairs of reverse plane partitions of shape $\lambda$ satisfying $g(\Lambda,\Lambda') = 0$. We have shown that this is equal to the RHS, which is now the generating function for reverse plane partitions of shape $\lambda$. □

## 4.3 Bijective Proof

Potentially break this proof up into various parts, add pictures, and reword things to make it potentially shorter The equivalence found in the previous section suggests that there might exist a nice bijection between pairs of RPPs each of shape $\lambda$ and with total volume $n$ and with no tile overlaps described in Figure 9, and single RPPs of shape $\lambda$ and total volume $n$. In this section, we describe such a bijection.

First, we can divide a partition into paths as follows. The first path begins in the top square of the leftmost column of the partition. This path moves to the right one square if possible, otherwise it moves down one square. If we remove all squares on this path from the partition, we are left with a strictly smaller partition. We can repeat this process until we are left with the empty partition.

**Example 20.** *We can associate the partition* $15 = 4 + 4 + 3 + 3 + 1$ *with paths:*

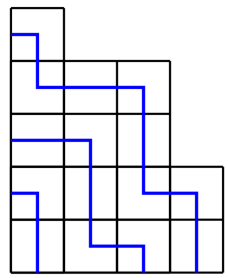

**Figure 10:** The path configuration for the partition $15 = 4 + 4 + 3 + 3 + 1$

We can think of these paths as the top view of stacks of blocks with paths on them. We can make each path connected by creating rules for drawing paths on lozenge tilings. In white columns of a lozenge tiling, we draw vertical paths on lozenges of orientation $a$ and upward diagonals on tiles $c_r$ and $c_l$. In gray columns, we draw vertical paths on lozenges of orientation $b$ and downward diagonals on tiles $c_r$ and $c_l$. We can also draw pairs of paths in this way for pairs of RPPs with the same shape.

**Example 21.** *We can associate an RPP with an arrangement of paths on the corresponding lozenge tiling:*

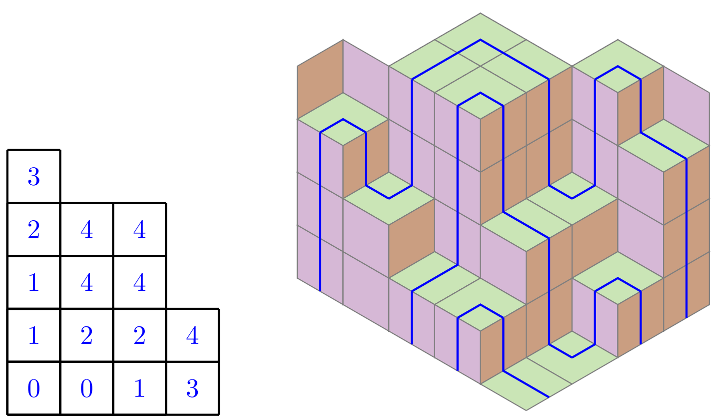


**Figure 11:** An RPP and the corresponding path configuration

**Example 22.** *We can associate a pair of plane partitions with a pair of paths on the corresponding overlaid lozenge tilings:*

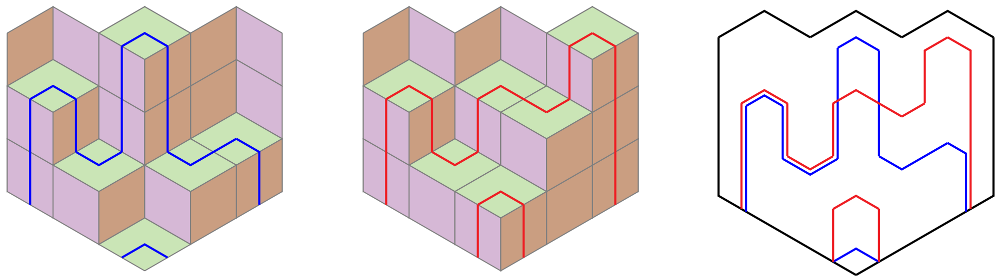

**Figure 12:** A pair of path configurations for two RPPs of the same shape

Using paths drawn in this way, the four tile interactions which contribute a nontrivial factor of $t$ correspond to the four path interactions shown below:

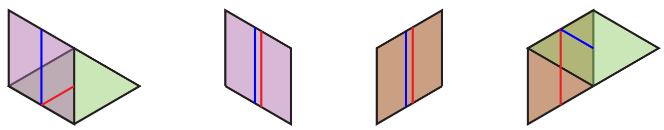

Then the weight of a pair of RPPs has no factor of $t$ if and only if it contains none of these path overlaps. We note that these disallowed overlaps contain both possible ways for a blue path and a red path to separate with a blue path on top.

We now investigate conditions that must be met for the weight of a pair of RPPs to have no factor of $t$. The top red path and the top blue path must start at the same spot and end at the same spot. Because these paths can never separate with the blue path on top, we determine that the top red path must always lie on or above the top blue path. Similarly, the second red path must lie on or above the second blue path, and so on through all paths.

Furthermore, because the top blue path ends above the second red path, the top blue path can never lie on or below the second red path, as this would require that they eventually separate with the blue path on top. Similarly, the second blue path must always lie strictly above the third red path, and so on through all paths.

Since paths drawn in this way are all separate on a single lozenge tiling, it is natural to try to create a single lozenge tiling by separating these paths. For instance, we can translate the top blue path down by 1 to separate it from the top red path. We must then translate the second red path down by 1 to keep it separate from the top blue path. We can then translate the second blue path down by 2 to separate it beneath the second red path, but then we must translate the third red path down by 2 as well. We can continue in this way through the entire partition, translating the $i$-th blue path and the $(i+1)$-th red path down by $i$.

**Example 23.** *We begin our bijection with a pair of RPPs with a weight not containing a factor of $t$.*

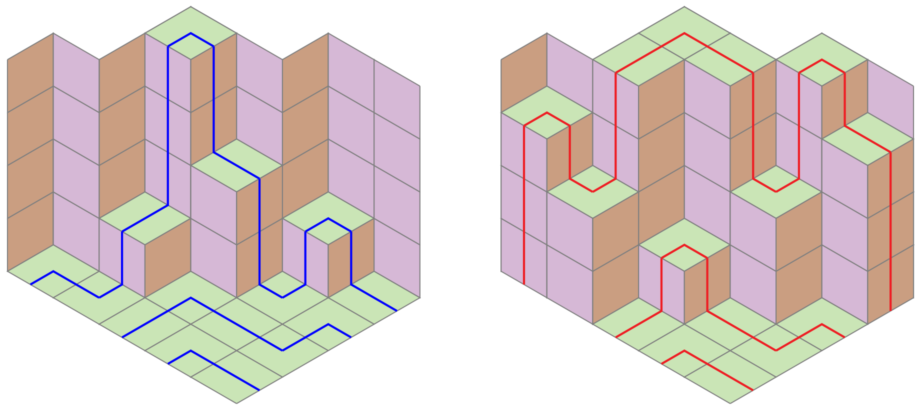

**Figure 13:** The path configurations for a pair of RPPs with a weight containing no factor of $t$

*We can now look at just the red and blue paths overlaid on top of each other. We separate the paths by sliding the first blue path down by 1, then sliding the second red path down by 1, then sliding the second blue path and third red path down by 2, then sliding the third blue path (and fourth red path, if it exists) down by 3, and so on, then removing the parts of the paths outside of our boundary.*

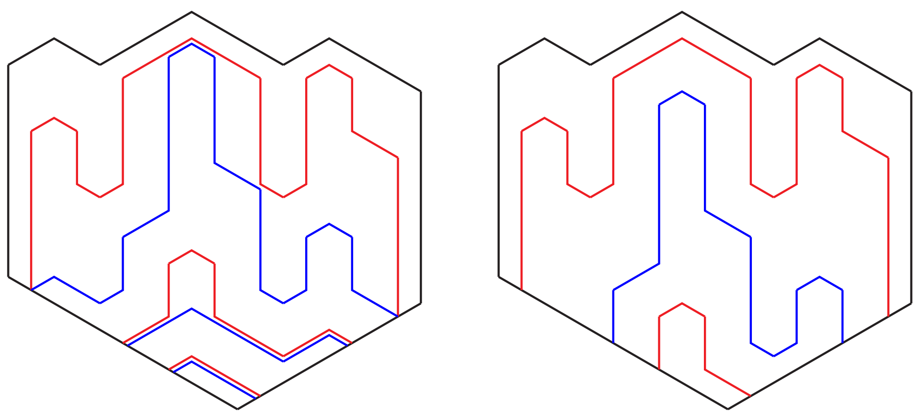

**Figure 14:** The pair of path configurations, and the corresponding path configuration after our transformation

*The newly constructed path configuration corresponds to a single lozenge tiling.*

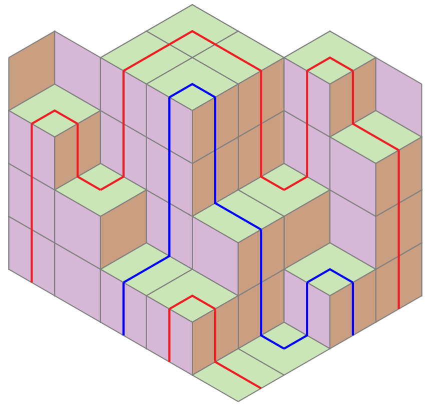

**Figure 15:** The lozenge tiling corresponding to our resulting path configuration

Translating down by 1 in a lozenge tiling corresponds to translating diagonally down and left by 1 in the "top view" Young diagram. Then this process results in a valid RPP if we can show that all of the nonzero boxes in the $(i+1)$st red path are outside of the first $i$ rows (from the bottom) and columns (from the left), and that all of the nonzero boxes in the $i$-th blue path are similarly outside of the first $i$ rows and columns, and all the necessary inequalities hold. We will show this inductively.

As a base case, all of the nonzero boxes in the 1st red path are outside of the first 0 rows and columns, since the entire path is outside of these 0 rows and columns. For the inductive step, we will show that the necessary conditions for the $(i+1)$st red path follow from the conditions for the $i$th blue path, then show that the necessary conditions for the $i$th blue path follow from the conditions for the $i$th red path.

Suppose that the first $i$ rows and columns of the $i$-th blue path are all 0 for some $i \geq 1$. We want to show that the first $i$ rows and columns of the $(i+1)$-th red path are all 0. We can in fact prove the stronger claim that the value in some box $x$ in the red RPP must be less than or equal to the values in any box in the blue RPP lying on a different path than $x$ and above $x$ or to the right of $x$. In other words, the $i$-th blue path and the $(i+1)$-th red path satisfy all of the necessary inequalities to be a RPP. This is stronger because the red path lies inside the blue path. Thus, if the first $i$ rows and columns of the blue path are 0, then the first $i$ rows and columns of the red path must also be 0 in order to be a RPP.

Consider two adjacent boxes on different paths in an RPP, where one box is above the other. Because these boxes lie on different paths, the blue path on the top box must exit to the right, and the red path on the bottom box must enter from the left. In the lozenge tiling, this corresponds to a white column with a blue $c_l$ and a red $c_r$. If the boxes contain the same value, then the $c_r$ is immediately below the $c_l$, and the red path is exactly 1 unit below the blue path. If the red box contains any larger number, the $c_r$ is higher up by at least 1, so the red path is on or above the blue path. This cannot be the case without adding a factor of $t$, because this blue path (path $i$) must end above this red path (path $i+1$). Thus, if this red path is ever on or above this blue path, then at some point the two paths must separate with the blue path on top, which contributes a factor of $t$.

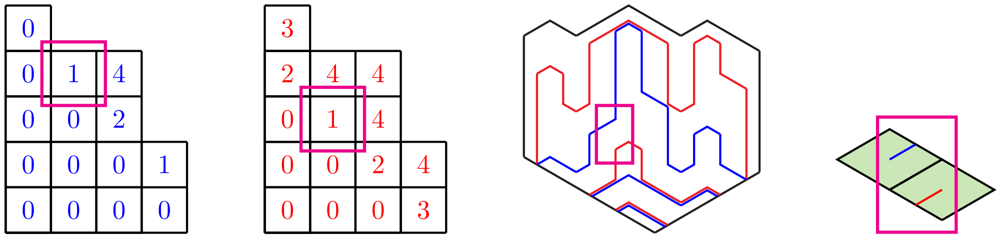


**Figure 16:** Hmmm, red boxes

We can also consider adjacent boxes on different paths in an RPP, where one box is to the right of the other. We can use a similar argument. Because these boxes lie on different paths, the blue path on the right box must enter from the top, and the red path on the left box must exit on the bottom. In the lozenge tiling, this corresponds to a gray column with a blue $c_r$ and a red $c_l$. If the boxes contain the same value, then the $c_l$ is immediately below the $c_r$, and the red path is exactly 1 unit below the blue path. If the red box contains any larger number, the $c_r$ is higher up by at least 1, so the red path is on or above the blue path. This cannot be the case without adding a factor of $t$, because this blue path (path $i$) must end above this red path (path $i+1$). Thus, if this red path is ever on or above this blue path, then at some point the two paths must separate with the blue path on top, which contributes a factor of $t$.

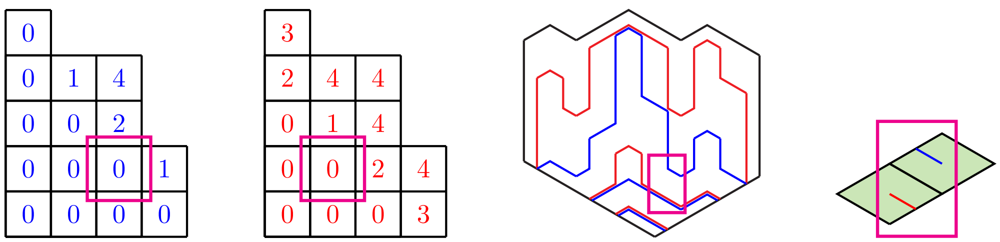


**Figure 17:** Wau more red boxes but in different places

This is half of our induction complete. If this process satisfies all properties of RPPs through the $i$-th blue path, then we also get the $(i+1)$-th red path and all properties of RPPs are still satisfied. We now want to show that if this process works through the $i$-th red path, then we also get the $i$-th blue path.

Specifically, we want to show that if the first $i-1$ rows and columns of the $i$-th red path are all 0, then the first $i$ rows and columns of the $i$-th blue path are all 0, and translating the blue path down by 1 results in a valid RPP consisting of these two paths. We can check this by showing that for any box $x$, the value in $x$ in the blue RPP must be less than or equal to the value in the red RPP of any box immediately left or down from $x$ and on the same path as $x$. This is because these boxes are immediately up and right, respectively, from the box where the blue value in $x$ will be translated to.

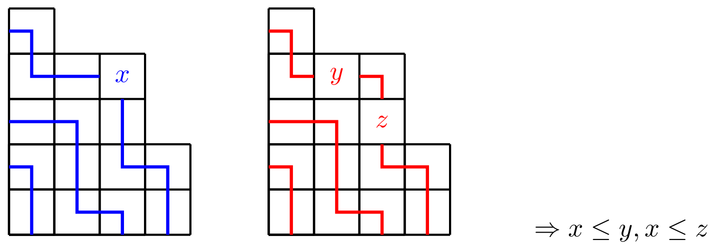

Figure 18: Double your luck

Proving this will also prove that the first $i$ rows and columns of the blue path are all 0, because we can add a column of all 0 at the left of each RPP and a row of all 0 at the bottom of each RPP, which only tiles of orientation $c$ to the lozenge tiling, resulting in no additional weight or interaction terms. Then any box of the $i$-th path in any of the $i$ leftmost columns in the new red RPP is 0, because each of these columns is all 0 in this path. Then the top box of the $i$-th path in any of the $i+1$ leftmost columns in the new blue RPP is 0. This is because the box is the topmost in this column and path, so the path must enter from the left, meaning the box to the left is in the same path. Then the box to the left is in one of the $i$ leftmost columns, so the red value is 0. In other words, if our claim is true, then all zeros and inequalities will be satisfied and this process will result in a valid RPP.

Consider two adjacent boxes on the same paths in an RPP, where one box is to the right of the other. Because these boxes lie on the same path, the blue path on the right box must enter from the left, and the red path on the left box must exit to the right. In the lozenge tiling, this corresponds to a white column with a blue $c_r$ and a red $c_l$. If the boxes contain the same value, then the $c_l$ is immediately below the $c_r$, and the red path exactly meets the blue path. If the blue box contains any larger number, the $c_r$ is higher up by at least 1. There are two cases here:

**Case 1:** If the blue path has a lozenge $a$ immediately above the red $c_l$, then any direction the red path takes contributes a factor of $t$.

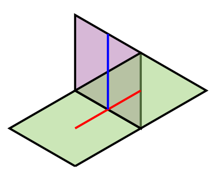

Figure 19: Possible red paths in Case 1

**Case 2:** If the blue path does not have a lozenge $a$ here, then it must have entered this column above the red path. This cannot be the case without adding a factor of $t$, because this blue path started in the same place as this red path. Thus, if this blue path is ever strictly above this red path, then at some point the two paths must separate with the blue path on top, which contributes a factor of $t$.

Now consider two vertically adjacent boxes on the same path in an RPP. Because these boxes lie on the same path, the blue path on the top box must exit to the bottom, and the red path on the bottom box must enter from the top. In the lozenge tiling, this corresponds to a grey column with a blue $c_l$ and a red $c_r$. If the boxes contain the same value, then the $c_r$ is immediately below the $c_l$, and the blue path exactly meets the red path. If the blue box contains any larger number, the $c_l$ is higher by at least 1. Again, there are two cases here:

**Case 1:** If the red path entered this column at or above the blue path, then there must be some red $b$ tiles to connect the red $c_l$ tile to the lower red $c_r$ tile. In particular, the top of one of these $b$ tiles coincides with the bottom of the blue $c_l$ tile, so either direction that the blue path can take contributes a factor of $t$.

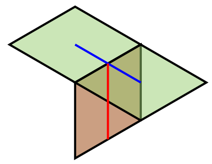

**Figure 20:** Possible blue paths in Case 1

**Case 2:** If the red path entered this column below the blue path, then in some column to the left of this, the blue path separated from the red path with the blue path on top, which must have contributed a factor of $t$.

In particular, if a box is nonzero in the blue RPP, then any box immediately to the left of this box or below this box on the same path in the red RPP must be nonzero. Because all of the nonzero boxes in the $i$th red path are outside of the first $i-1$ rows and columns, all of the nonzero boxes in the $i$th blue path must be outside of the first $i$ rows and columns.

We then conclude that if two RPPs of the same shape have no bad overlaps, then this process will result in a single valid RPP with the same shape. We now must show that every valid RPP can be obtained in this way.

For any RPP, we can examine the lozenge tiling and draw paths as above. In a single RPP, we can draw paths as described above, alternately coloring the paths red and blue, starting by coloring the top path red. We can then reverse our transformation, packing the red paths into one RPP and the blue paths into another RPP. We can then fill in the rest of these RPPs with 0s.

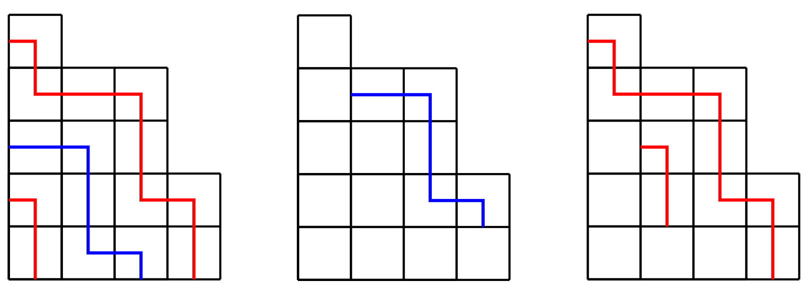

**Figure 21:** We can decompose any RPP into a pair of RPPs with no factor of $t$ in their weight by reversing our transformation

We can similarly draw our alternately-colored paths on the single lozenge tiling corresponding to our single RPP. Because we are not overlapping tiles, no two paths ever touch. We can then translate the $i$-th blue path and the $(i+1)$-th red path up by $i$ for $i \in \{1, 2, \dots\}$.

The $i$-th blue path always is translated up by 1 relative to the $i$-th red path, and if we look at the preimage of any bad overlap under this transformation, we see that the paths are not separate. Because we began with separate paths from our single RPP, the resulting pair of RPPs cannot have any bad overlaps.

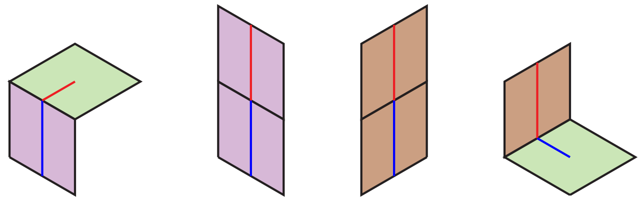

**Figure 22:** The preimages of bad overlaps under our transformation

As a result, every RPP can be obtained via this process from two RPPs with no factor of $t$. As we showed before, this process always results in a valid RPP, so this is in fact a bijection. In other words, there are exactly as many pairs of RPPs with shape $\lambda$ and total volumne $n$ and no bad overlaps as there are RPPs with shape $\lambda$ and volume $n$.

# 5 Additional Information

## 5.1 More Than Two Colors

As alluded to previously in the colored vertex model section (2.2), we can expand our vertex model to $k$-colors.

Call the colors $c_1, \dots, c_k$ and order them such that $c_i < c_j$ if and only if $i < j$. In this case, we have

$$L_{x;t}^{(k)}(\vec{v}) = \prod_{i=1}^{k} L_{xt^{\delta_i}}(v_i), \qquad \delta_i = \#\{j > i \text{ s.t color } j \text{ is present}\}$$

$$(L')_{x;t}^{(k)}(\vec{v}) = x^k t^{\binom{k}{2}} L_{\bar{x};t}^{(k)}(\vec{v}), \qquad \bar{x} = \frac{1}{xt^{k-1}}$$

$$R_{z;t}^{(k)}(\vec{v}) = \prod_{i=1}^{k} R_{z/t^{r_i}}(v_i), \qquad r_i = \#\left\{ j > i \text{ such that color } j \text{ looks like } \right\}$$

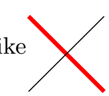

Something something about results when we take extra colors. We don't actually need to write this out completely, this thought it could be added as like some extra stuff to think about

# References


[1] A. Aggarwal, A. Borodin, and M. Wheeler. Colored fermionic vertex models and symmetric functions. *Communications of the American Mathematical Society*, 3(08):400–630, 2023.

[2] K. Andrews, G.E. Eriksson. *Integer Partitions.* Cambridge University Press, 2004.

[3] A. Borodin and V. Gorin. Lectures on integrable probability. *Probability and statistical physics in St. Petersburg*, 91:155–214, 2016.

[4] C. Boutillier, J. Bouttier, G. Chapuy, S. Corteel, and S. Ramassamy. Dimers on rail yard graphs. *Annales de l'Institut Henri Poincaré (D) Combinatorics, Physics and their Interactions*, 4(4):479–539, 2017.

[5] S. Corteel, A. Gitlin, D. Keating, and J. Meza. A vertex model for LLT polynomials. *International Mathematics Research Notices*, 2022:15869–15931, 2022.

[6] N. Reshetikhin. Lectures on the integrability of the six-vertex model. 2010.

[7] R. Stanley. Theory and applications of plane partitions. part 2. *Stud. Appl. Math.*, 50:259–279, 1971.

[8] R. Stanley. *Enumerative Combinatorics*, volume 2. Cambridge University Press, 1999.